

# Snowmelt Runoff Modelling under Projected Climate Change Patterns in the Gilgit River Basin of Northern Pakistan

Muhammad Adnan<sup>1</sup>, Ghulam Nabi<sup>2</sup>, Shichang Kang<sup>1,3\*</sup>, Guoshuai Zhang<sup>4</sup>,  
Rana Muhammad Adnan<sup>5</sup>, Muhammad Naveed Anjum<sup>6,7</sup>,  
Mudassar Iqbal<sup>8</sup>, Ayaz Fateh Ali<sup>1</sup>

<sup>1</sup>State Key Laboratory of Cryospheric Sciences, Northwest Institute of Eco-Environment and Resources, Chinese Academy of Sciences (CAS), Lanzhou 730000, China

<sup>2</sup>Centre of Excellence in Water Resource Engineering, University of Engineering and Technology Lahore, 54000, Pakistan

<sup>3</sup>CAS Center for Excellence in Tibetan Plateau Earth Sciences, Beijing 100101, China

<sup>4</sup>Key Laboratory of Tibetan Environment Changes and Land Surface Processes, Institute of Tibetan Plateau Research, Chinese Academy of Sciences, Beijing 100085, China

<sup>5</sup>School of Hydropower and Information Engineering, Huazhong University of Science and Technology, Wuhan 430074, China

<sup>6</sup>Key Laboratory of Inland River Eco-hydrology, Northwest Institute of Eco-Environment and Resources, CAS, Lanzhou 730000, China

<sup>7</sup>University of Chinese Academy of Sciences, Beijing 100049, China

<sup>8</sup>Key Laboratory of land Surface Process and Climate Change, Northwest Institute of Eco-Environment and Resources, Chinese Academy of Sciences, Lanzhou 730000, China

*Received: 7 September 2016*

*Accepted: 3 November 2016*

## Abstract

Pakistan is home to three of the world's largest mountain ranges in the Upper Indus Basin (UIB), where the majority of Pakistan's water resources are located: the Himalayan, Karakorum, and Hindu-Kush. This work estimated the (snow+glacier) and rainfall runoff from one of the major tributaries, the Gilgit River, nestled within the UIB of Pakistan. The snowmelt runoff model (SRM) derived by the cryospheric data from the MODIS (moderate resolution imaging spectroradiometer) was employed to predict the daily discharges of the Gilgit. The SRM was successfully calibrated, and the simulation was undertaken from 2005 to 2010, with a coefficient of model efficiency ranging from 0.84-0.94. The average contributions of (snow+glacier) and rainfall to the stream flows of the Gilgit from 2001-10 were 78.35% and 21.65%, respectively, derived from the SRM. The representative concentration pathways (RCP) 4.5 and 8.5 scenarios of the Intergovernmental Panel on Climate Change (IPCC) AR5 were used to investigate the effects of the changes in temperature on climate of the Gilgit catchment. Under the RCP 4.5 scenario, the air temperature

of Gilgit will increase by 3°C, whereas the increase in precipitation will be minor. Under the RCP 8.5 scenario (overshooting scenario), air temperature will increase by 10.7°C, whereas precipitation will decrease between 2010 and the end of the 21<sup>st</sup> century in the Gilgit catchment. The application of the RCP 4.5 and 8.5 mean temperature scenarios in the SRM suggested that with increases in mean temperature of 3.02°C and 10.7°C, respectively, the average annual runoff in the Gilgit will increase by 67.03 and 177.5%, respectively, compared with the observed runoff by the end of the 21<sup>st</sup> century. This increased surface runoff from snow/glacier melt can potentially be utilized by planning new storage areas at appropriate locations to harness additional water.

**Keywords:** snowmelt runoff model, climate change, RCP, trend analysis, Upper Indus Basin

## Introduction

Pakistan has a surface water-driven economy, and the water available through the long Indus Basin River System is largely consumed by the agricultural sector. The flows in the Indus Basin River System are mainly dependent on the snow/glacier melt in the northern regions of Pakistan, which forms the upper catchments and includes three of the world's largest mountain ranges: the Himalayan, Karakoram, and Hindu-Kush (HKH). A major part of the flow extracted from the Indus at Tarbela Dam is contributed by snow- and glacier melt of the HKH mountain ranges [1-3]. The contribution of the flow from the Upper Indus Basin (UIB) is more than 70%, and it originates from zones of heavy snowfall situated above 4,000 m elevation, as reported in other studies [4-5]. Approximately 50% of the runoff, as a fraction of the total annual discharge, is due to snowmelt from the Western Himalayan catchments [1, 5]. The maximum precipitation in the UIB occurs during the winter and spring seasons due to the westerlies [6-7].

The HKH region temperature has warmed by approximately 1.5°C, which is almost double the amount in other parts of Pakistan (0.76°C) during the last 30 years [8]. A significant increase in the temperature of the HKH region is expected to impact snow cover dynamics, which in turn will affect seasonal flow variations [3, 9-10]. The Western Himalayas have experienced a substantial surge in seasonal mean minimum temperature [11]. Summer cooling and winter warming trends have been detected over the Bunji and Gilgit climatic stations [12]. Researchers agree that the glaciers have slightly expanded and shown positive mass balance in the Karakoram region since the beginning of the 21<sup>st</sup> century [13-15]. However, in the Trans-Himalayas, decreases in the glacier area were observed from 1969 to 2010 [16]. Most of the glaciers in the HKH region have been declining and losing their mass since 1950, but the observed variations are not regionally uniform [12, 17-18]. Glacier fluctuations in the UIB are most likely due to precipitation rather than thermal anomalies [19].

The unprecedented melting of the Himalayan glaciers would likely cause extreme flooding, followed by reduced river flows, in the next two to three years [20]. The impact of climate change on runoff is more adverse, especially in snow-fed rivers [21-22]. Significant decreasing trends in

summer and increasing trends in winter in mean monthly flow were observed at eight stream gauging stations located in the UIB [23]. The analysis of the observed annual average discharge from 2001-05 showed that the contribution of precipitation to the average annual discharge was less than that of snowmelt due to enhanced glacier melting in the UIB [10].

The topography and climate of the mountainous area have caused strong variations in glacier behaviour, and it has become difficult to understand the climate change impacts in the HKH region [24]. In the HKH region, there is also the problem of scarcity of hydrological, meteorological, and glaciological data due to difficult terrain [25-26], which prevents an understanding of the main characteristics of the hydrological processes that control runoff generation at high elevation basins [18]. An energy balance model is ideal for understanding the melting processes of snow and glaciers, but it requires much data that are mostly unavailable in high elevation mountainous regions [27-28]. Mass balance studies methods were found to be complex and time-consuming [29-30].

At present, limited work has been conducted to account for the river runoff fluctuations in response to changing climate, and few studies are available in which different runoff components of streams flows were quantified in the HKH region. The Gilgit River basin was selected as the study area due to its location in a higher elevation range (1,415 m to 7,104 m a.s.l.) within the UIB. The Gilgit basin is snow fed, and reasonably larger datasets were available for this area. Approximately 50,000 MW of hydropower potential was identified in the UIB; thus, any change in available water would have negative impacts on power generation, as well as on agriculture and the livelihood of downstream areas. This work aimed to quantify future available water resources using a temperature index modelling approach on the Gilgit basin under RCP emission scenarios taken from the IPCC AR5. The Snowmelt runoff model was applied over the Gilgit basin, and future flows were predicted under the RCP 4.5 and 8.5 emission scenarios from 2011 to 2100 using mean temperature. Another objective of this study was to estimate the relative contributions of discharge components to stream flow for rainfall and snow/glacier melt separately by using the SRM.

### Snowmelt Runoff Model

Different hydrological models were previously used to account for discharge simulations in a basin where snow and glacier melt made major contributions to stream flow [9, 31-34]. The modelling of snow- and glacier melt varies from simple to complex. On this basis, the Snowmelt Runoff models were divided into two categories: energy-based models and temperature index models [31]. The large amounts of data required for energy-based models are usually not available in high elevation catchments. In the temperature index approach, the overall melt rate is considered proportional to the air temperature, the proportional factor is called the melt factor, and the air temperature is expressed as degree days. This approach is flexible, and basic meteorological data are used as the input for driving the model. The Snowmelt Runoff Model (SRM) is also based on the temperature index approach. The SRM has been widely used in various parts of the world. [35] explained the topographic effects on complex terrain with limited input data using the SRM, and [36] used the SRM to estimate the climate-affected runoff in the Ganga and Brahmaputra rivers. The SRM was used for the estimation of snowmelt runoff for hydropower generation and water management in the non-monsoon season [37].

The SRM was used for flood forecasting and management of the Swat River basin [38], and [39] used the SRM in the Kuban River basin using MOD10A2 satellite data. [22] applied the SRM for snowmelt runoff modelling in the Tamor River basin in the eastern Nepalese Himalayas. The purpose was to study the variations in hydrological processes due to climate change. The SRM was used for the prediction of future flows under different climate change scenarios in the Hunza River basin in Pakistan [40]. The most common expression related to snowmelt and temperature index is given below in Equation (1):

$$M = D_f (T_i - T_b) \quad (1)$$

...where  $M$  is the depth of melt water in (cm),  $D_f$  is the degree day factor ( $\text{cm } ^\circ\text{C}^{-1}\text{d}^{-1}$ ),  $T_i$  is the index air temperature ( $^\circ\text{C}$ ), and  $T_b$  is the base temperature ( $^\circ\text{C}$ ).

The SRM was developed by Martinec in 1975 and was successfully tested [34, 41]. This model is suitable where snow is a major contributor to stream flow. Due to the recent availability of high resolution cryosphere data, the SRM can be applied to a large size basin. It can be applied to basins of any size and at any elevation range. The SRM was applied in an arid mountain watershed with limited hydro-meteorological data. It was observed that the degree day factor varied on the basis of shortwave radiation and snow albedo [42]. Variation in the hydrological process due to climate change should be studied on finer basin scales for the assessment of water availability and vulnerability [22]. The basic input data required for the SRM are daily temperature, daily precipitation, daily discharge data, and snow cover percentage values. After

considering the variables, nine parameters, including temperature lapse rate, critical temperature, degree day factor, lag time, snow/rainfall runoff coefficients, rainfall contributing area, and recession's coefficients ( $X_c$  and  $Y_c$ ) were used for the calibration of the SRM model. Some information about basin characteristics is also required, such as basin area, zone area, and the mean hypsometric elevation of each zone. In the model, snowmelt and rain are computed every day and then superimposed on the calculated recession flow and transformed into the daily discharge from the catchment. In this study, the critical temperature ( $T_{crit}$ ) was used as a threshold to differentiate between rain and snow. Precipitation was considered as snow in the model when  $T < T_{crit}$  and vice versa.

The main equation used in the SRM for the snowmelt runoff simulation is given below:

$$Q_{n+1} = [c_{Sn} a_n (T_n + \Delta T_n) S_n + c_{Rn} P_n] \frac{A * 10000}{86400} (1 - k_{n+1}) + Q_n k_{n+1} \quad (2)$$

... where  $Q$  is the average daily discharge ( $\text{m}^3\text{s}^{-1}$ ),  $C_s$  is the coefficient of snow,  $C_r$  is the coefficient of rain,  $a$  is the degree day factor ( $\text{cm } ^\circ\text{C}^{-1}\text{d}^{-1}$ ),  $T$  is the number of degree days ( $^\circ\text{C d}$ ),  $S$  is the ratio of snow-covered area to total area,  $P$  is the precipitation contributing to runoff (cm),  $A$  is the area of the basin or zone ( $\text{km}^2$ ),  $k$  is the recession coefficient indicating the decline in discharge, and  $n$  is the sequence of days during the discharge computation period. This detailed description of the parameters was given by [43].

The efficiency of SRM can be evaluated using two criteria:

1. Coefficient of determination,  $R^2$
2. Volume difference,  $D_v$  %

The formulas for these factors are given in equations 3 and 4, respectively,

$$R^2 = 1 - \frac{\sum_{i=1}^n (Q_i - Q_i')^2}{\sum_{i=1}^n (Q_i - \bar{Q})^2} \quad (3)$$

...where  $R^2$  is the measure of model efficiency,  $Q_i$  is the measured daily discharge ( $\text{m}^3/\text{s}$ ),  $Q_i'$  is the simulated daily discharge,  $\bar{Q}$  is the average daily discharge for the simulation year, and  $n$  is the number of daily discharge values.

$$D_v = \frac{VR - VR'}{VR} * 100 \quad (4)$$

...where  $D_v$  is the percentage difference between the total measured and simulated runoff,  $V_R$  is the measured runoff volume, and  $V_R'$  is the simulated runoff volume.

The SRM can also be used to predict future stream flows under certain temperature and precipitation climate change scenarios. [36] carried out a study of snow cover

mapping to monitor the climate affected runoff in the Ganga and Brahmaputra rivers. The climate change scenario in the SRM was used to calculate climate-affected flow. [44] studied the prediction of snow cover, glaciers, and runoff in a changing climate. It was reported that the SRM can be used efficiently for short- and medium-term runoff forecasting [39, 45]. Previous studies showed that the SRM can be used successfully in snow and glaciated basins.

## Material and Methods

### Characteristics of the Study Area

The Gilgit River is situated at high altitudes in the Himalaya-Karakorum-Hindu Kush (HKH) region. It originates from Shandoor Lake, which is located in the Gilgit-Baltistan region of northern Pakistan. The lake is nested in the Hindu-Kush mountainous range with average elevation of about 3,738 m.a.s.l. The present study area lies between latitude  $35^{\circ}46'05''$  N to  $36^{\circ}51'16''$  N and longitude  $72^{\circ}25'02''$  E to  $74^{\circ}19'25''$  E. Baha Lake is the main right bank tributary of the Gilgit River, which is located near the Handrab and Langar rivers. Some small rivers like the Yasin, Phandar, and Ishkoman drain into

the Gilgit from the left bank. The Phandar River joins the Gilgit near Phandar Lake, located in Ghizer. The Yasin joins the Gilgit at the point of Gupis. The snow and glacier meltwater from the Karakoram and Hindu-Kush ranges feed the Gilgit [46].

The Gilgit flows from west to east and enters Gilgit District and then ultimately empties into the Indus River. The catchment area of the Gilgit basin at Gilgit stream gauging station is approximately 12,671 km<sup>2</sup>, extracted from the SRTM 90 m DEM. The total number of glaciers in this catchment is 923, covering an area of 858.168 km<sup>2</sup> [25]. The study area is shown in Fig. 1a). This area falls in the cold desert climatic regime. The average elevation of the Gilgit catchment is about 3,997 m.a.s.l. The southern part of the catchment receives a maximum amount of rainfall of about 1,000 mm/year, while the amount of rainfall in agricultural areas is less than 500 mm/year. The broad tract of the Gilgit River receives about >125 mm/year of rainfall. The altitude (1,250 to 8,611 m.a.s.l) also affects the climate of the Gilgit-Baltistan region. The lower elevation valleys are characterized as arid while high-altitude valleys are semi-arid. Usually, the maximum temperature in high-altitude valleys located in Gilgit catchment is 10-15°C – higher than those located at Astore, Ganche, Skardu, and Hunza-Nagar [47]. The Gilgit hydrological station is situated at an elevation of

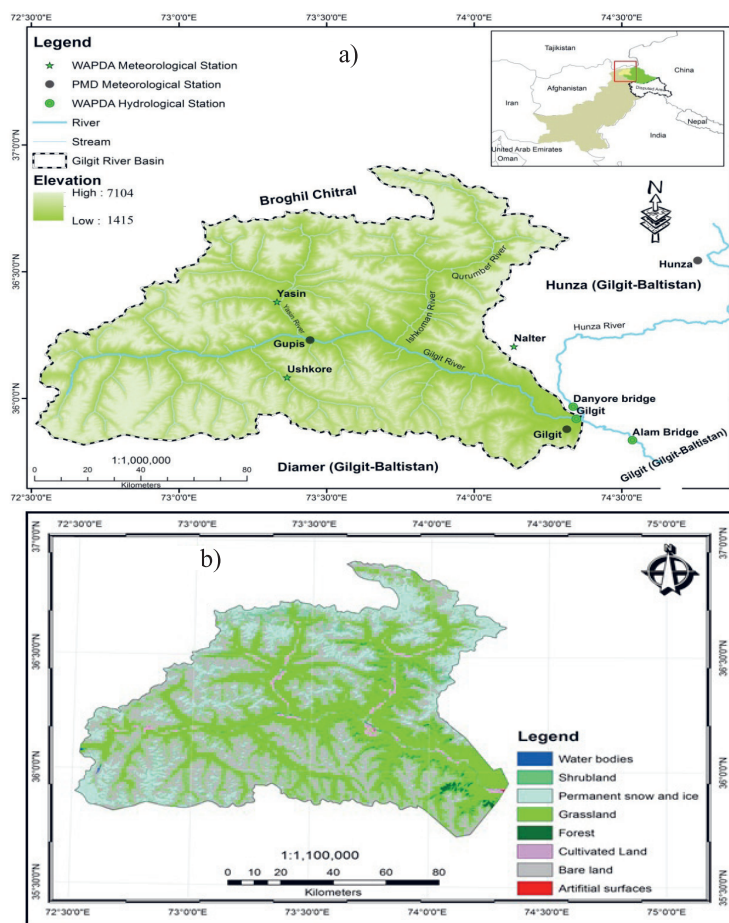


Fig. 1. a) Geographical map of Gilgit catchment, b) land use map of Gilgit catchment.

1,430 m. The Gilgit has a mean annual discharge (at Gilgit stream gauging station) of 288.63 m<sup>3</sup>/s according to the 50-yr (1961-2010) record. Gilgit catchment includes four climatic stations: Gilgit, Gupis, Yasin, and Ushkore. Mean annual total precipitation is 132 mm, 314 mm, and 311 mm in Gilgit, Yasin, and Ushkore, respectively. The average annual temperature at Gilgit, Gupis, Ushkore, and Yasin climatic stations is 15.99°C, 12.8°C, 6.02°C and 4.91°C, respectively, according to the seven-year record (2001-07). The precipitation lapse rate between low (1,460 m) and high (3,150 m) altitude climatic stations varies from season to season. In summer (April to June) it varies from 0.057 mm/100 m to 0.0002 mm/100 m. In winter, the value of precipitation lapse rate is higher in December (about 0.76 mm/100 m). The average annual precipitation lapse rate from low to high climatic stations is about 0.506 mm/100 m. The Gilgit flows in summer (June-September) are mainly affected by snow- and glacier melt [40].

Most of the catchment area of Gilgit consists of bare land (43.8%) and grass land (42.9%). The area covered by permanent snow and ice is approximately 12.7%. However, the cultivated and forest areas are small – approximately 1.95% and 1.30%, respectively (Fig. 1b).

### Data Sets

#### *Hydro-Meteorological Data*

The Pakistan Meteorological Department (PMD) collected the climatic data of the Gilgit station on a daily basis from 1975-2010 and on an annual basis from 1961-2010. Two high elevation stations, Yasin (3,150 m) and Ushkore (2,970 m), were installed by the Water and Power Development Authority (WAPDA). Records are available from 1999 onward. The data from these two climatic stations (1999 to 2010), collected on a daily basis, were used in the calibration of the snowmelt runoff model (SRM). The Surface Water Hydrology Project of the Water and Power Development Authority (SWHP-WAPDA) collected streamflow data on a daily basis from 1961-2010.

#### *Spatial Data*

The shuttle radar topography mission (SRTM) digital elevation data are generated by the U.S. National Aeronautics and Space Administration. The Gilgit Basin was delineated in ARC GIS using SRTM-DEM of 90 m resolution. The elevation range of the Gilgit catchment ranged from 1,415-7,104 m. The DEM after delineation was classified into six elevation zones with equal interval of 1,000 m. The DEM was reclassified into different elevation zones to estimate snow cover area variability with respect to elevation. The reclassified DEM is shown in Fig. 2 and description of elevation zones is given in Table 1.

Most of the area of the Gilgit watershed, approximately 6,806 km<sup>2</sup> or 53.71%, lies between the elevation

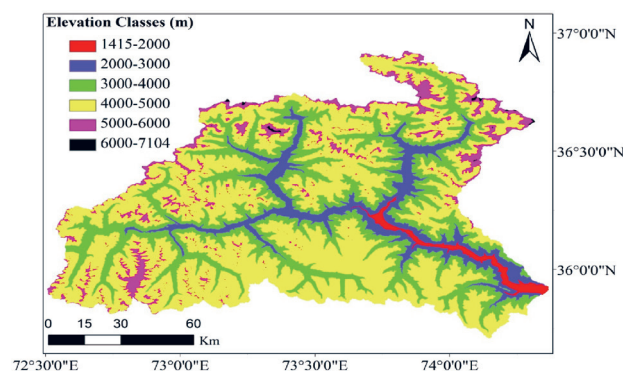


Fig. 2. Classification of digital elevation model with respect to elevation.

Table 1. Catchment area under different elevation zones.

| Zone | Elevation Classes (m) | Mean Elevation (m.a.s.l.) | Area (km <sup>2</sup> ) | % of Total Area |
|------|-----------------------|---------------------------|-------------------------|-----------------|
| A    | 1,415-2,000           | 1,730                     | 200                     | 1.58            |
| B    | 2,000-3,000           | 2,500                     | 1,247                   | 9.84            |
| C    | 3,000-4,000           | 3,500                     | 3,525                   | 27.81           |
| D    | 4,000-5,000           | 4,500                     | 6,806                   | 53.71           |
| E    | 5,000-6,000           | 5,500                     | 877                     | 6.92            |
| F    | 6,000-7,104           | 6,552                     | 16                      | 0.126           |

range of 4,000-5,000 m, and approximately 7.04% of the catchment area lies above 5,000 m elevation, above which most of the area is covered by perennial, non-perennial, permafrost, and glaciers with sparse vegetation and range lands.

#### *MODIS Satellite Data*

Daily moderate resolution imaging spectroradiometer (MODIS) terra data were downloaded to estimate the snow cover area variation in the Gilgit catchment. Ten-year data (2001 to 2010) collected on a daily basis and 12-year (2001 to 2012) data collected on a weekly basis (MOD10A2) were downloaded from the National Snow and Ice Data Center (NSIDC; [nsidc.org/data/modis/order\\_data.html](http://nsidc.org/data/modis/order_data.html)). The snow cover area values, known as the conventional depletion curve (CDC), were used as inputs in the SRM to estimate the snow/glacier melt runoff contribution into the Gilgit. The MODIS data were processed in Arc GIS. The CDC values for each elevation zone were computed and then used in the model as input to estimate the snowmelt runoff from each elevation zone separately. Before the computation of CDC values, snow cover area on nearly cloud-free Landsat7 ETM+SLC images was compared with the MODIS images on the same date to validate the

MODIS product. The normalized difference snow index (NDSI) approach was used to differentiate snow from its surrounding features. This approach uses shortwave near infrared bands to identify the snow. Snow has reflectance in band 4 and is low in band 6. The equation of NDSI is given below:

$$\text{NDSI} = (\text{band 4} - \text{band 6}) / (\text{band 4} + \text{band 6}) \quad (5)$$

The NDSI threshold of the MODIS snow cover products issued by the NSIDC is 0.40 [48]. The threshold value for the MODIS algorithm is 0.4; if  $\text{NDSI} > 0.4$  then it is snow, otherwise it is something else. The Landsat and MODIS images of 11 April 2000 and 7 October 2001 were selected for comparison. Two images, one in summer and the second in winter, were selected to check the MODIS performance in both seasons. In summer, the difference of snow cover area between the two products was only 0.54% while in winter the difference was 2.3%. The MODIS images with snow cover percentages greater than the corresponding cloud cover percentages were selected for further calculations. The images with a snow cover percentage of approximately 70% compared with cloud cover were considered reliable and were used in the analysis. A comparison of Landsat and MODIS images showed nearly the same snow cover area in the Gilgit catchment. Therefore, the validated MODIS snow images were used in this study. The data gaps produced due to cloudy images were filled using the linear interpolation method. In previous studies, MODIS satellite products were widely used all over the world to estimate the snow cover areas in high elevation basins [39, 49]. [40] validated a cloud-free

MODIS image with an ASTER image on the same date in the Hunza River basin, which is near the Gilgit River basin. The validation was performed on both the basin and the zone-wide snow cover areas of the images. The results showed that MODIS products are reliable for estimating snow cover areas in high elevation basins, such as the Hunza River basin and the basin-wide variations in the snow cover areas of Gilgit catchment (Fig. 3). The MODIS (MOD10A2) eight-day snow cover product was used for this study. Snow cover area was estimated at the start of each month. The average percentage of snow and ice cover area varies from 96% in the first week of January to 91% in the first of February. Almost all seasonal snow cover disappeared in July. In August, the ice and glacier cover area drop to 14%. From September, the snow cover area starts increasing and it again reaches 90-92% in December (Fig. 3).

#### Analysis of Temporal Changes in Climatic Data (1961-2010)

The long-term record of the Gilgit climatic station was available, and a trend analysis of the climatic data from 1961 to 2010 was performed. Double mass curve analysis was carried out to check the consistency of available meteorological data. Average annual meteorological data of Gilgit station from 1961 to 2000 was plotted against the average of five nearby climatic stations: Gupis, Astore, Bunji, Chilas, and Chitral. Results of the double mass curve of all stations and variables were straight lined and no break points were detected in time series data. Therefore, the observed climatic data was considered reliable for climate change studies and also for trend analysis. [50] also

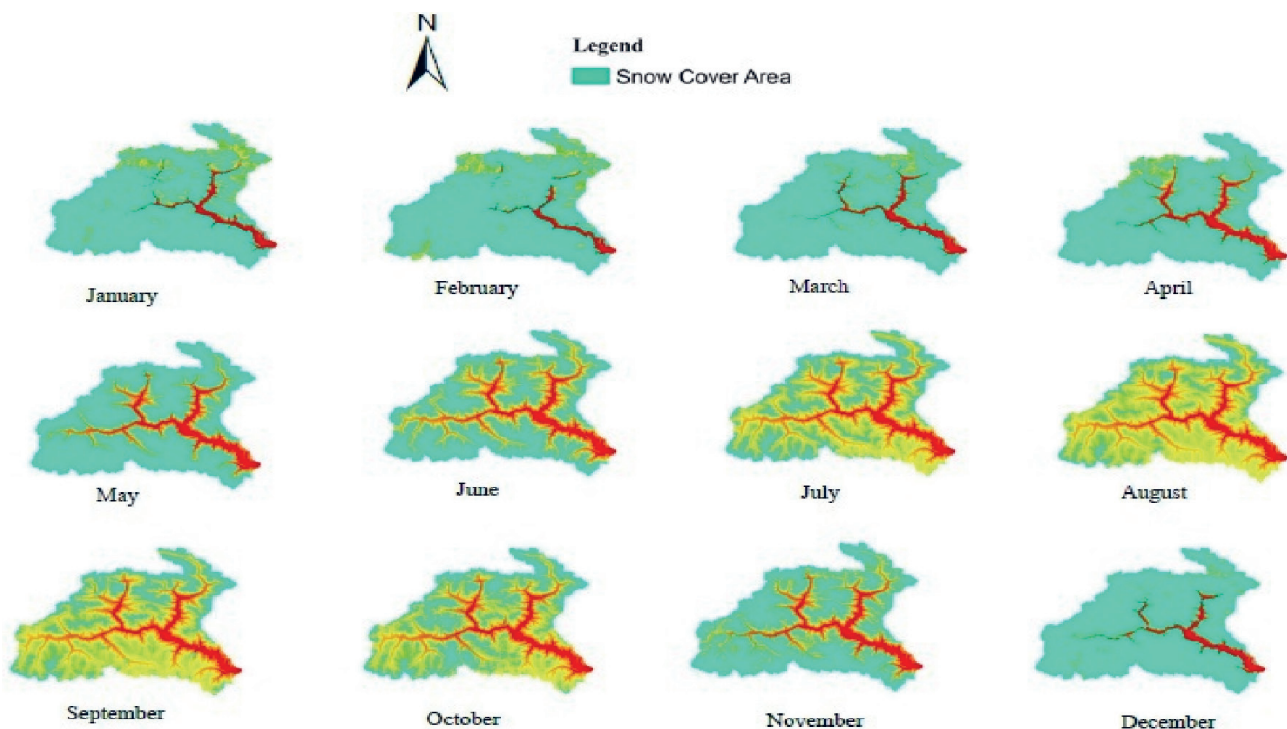


Fig. 3. Monthly snow cover area variations for 2009 in Gilgit catchment.

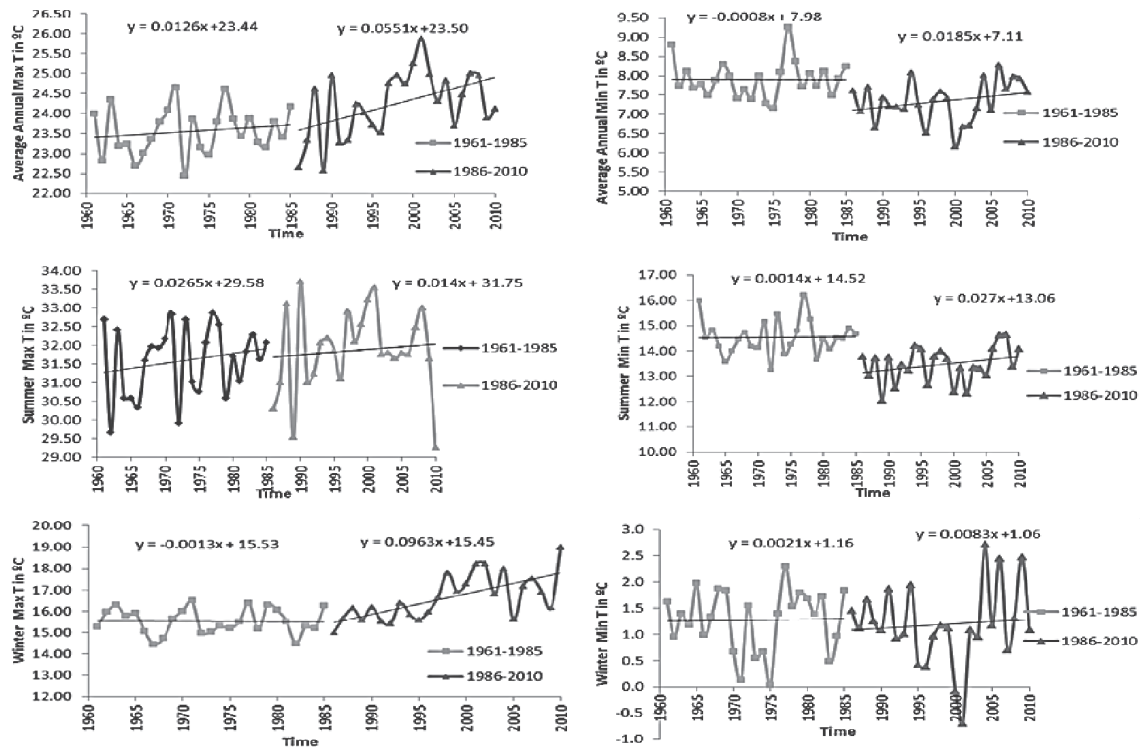


Fig. 4. Annual and seasonal trends of maximum and minimum temperatures of Gilgit station (1961-85 and 1986-2010).

used this technique to check the consistency of available meteorological data in yellow river source region. The results of all stations were straight line. The significance of the trends was found via Mann-Kendall trend analysis. Sen’s slope method was employed to estimate the slopes of the trends. These two methods were found to be useful in analysing the trends in climatic data.

### Maximum and Minimum Temperatures

The 50-year climatic data of the Gilgit catchment were analysed, and the results showed that rapid change occurred in climatic variables after 1985. On this basis, the

data were divided into two groups to check the variability during the first 25 years (1961 to 1985) and the second 25 years (1986 to 2010). The overall trend in the climatic data from 1961 to 2010 was also mapped, and the change in temperature is described (Table 2). The trends in average annual, summer, and winter maximum and minimum temperatures are shown (Fig. 4).

There were fewer changes in the annual, summer, and winter maximum temperatures from 1961 to 1985, but sudden increases were observed after 1985 (Fig. 4). This was due to global warming in Pakistan, and Pakistan was listed among the countries that are more vulnerable to climate change [51].

Table 2. Change in annual and seasonal maximum and minimum temperatures (°C) per period of the Gilgit climatic station using Mann-Kendall and Sen’s slope method.

| Seasons      | Maximum Temperature |         |                    | Minimum Temperature |         |                    |
|--------------|---------------------|---------|--------------------|---------------------|---------|--------------------|
|              | 1961-2010           | 1961-85 | 1986-2010          | 1961-2010           | 1961-85 | 1986-2010          |
| Annual (J-D) | <b><i>1.40</i></b>  | 0.38    | <b><i>1.36</i></b> | <b><i>-0.69</i></b> | 0.08    | 0.53               |
| Winter (O-M) | <b><i>1.93</i></b>  | 0.00    | <b><i>2.57</i></b> | 0.21                | 0.01    | 0.02               |
| Summer (A-S) | 0.77                | 0.58    | 0.77               | <b><i>-1.31</i></b> | 0.22    | 0.52               |
| Winter (DJF) | <b><i>2.19</i></b>  | -0.06   | <b><i>2.07</i></b> | 1.15                | 0.32    | 0.28               |
| Spring (MAM) | <b><i>2.25</i></b>  | 0.96    | <b><i>3.40</i></b> | 0.00                | 0.33    | <b><i>1.40</i></b> |
| Summer (JJA) | -0.42               | 0.40    | -0.03              | <b><i>-1.98</i></b> | 0.06    | 0.42               |
| Autumn (SON) | <b><i>1.55</i></b>  | -0.16   | 0.67               | <b><i>-1.11</i></b> | -0.27   | 0.03               |

Note: Bold and italic values show that the trend is significant at the 95% confidence level.

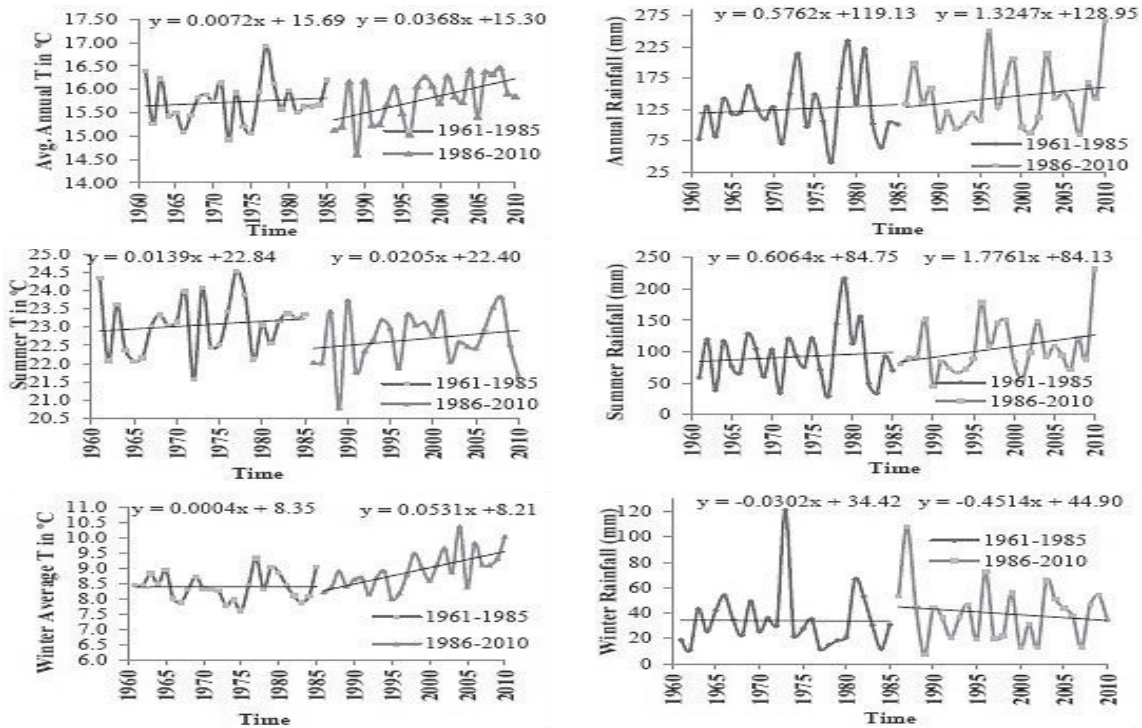


Fig. 5. Annual and seasonal trends of average annual temperatures and rainfall of Gilgit station (1961-85 and 1986-2010).

### Mean Temperature and Precipitation

Mann-Kendall trend analysis and Sen’s slope method were employed to account for the changes in annual and seasonal climatic parameters. The previous data analysis revealed significant changes in the climatic parameters of the Gilgit catchment, especially after 1980. Therefore, trend detections were performed on both short- and long-term bases. For this purpose, the 50-year time period was divided in two time periods to detect the trends before and after climate change, as well as overall. The trend analysis was performed on three periods, from 1961 to 2010, 1961 to 1985, and 1986 to 2010 (Table 3) and (Fig. 5). The trend

analysis revealed that the changes in mean and seasonal temperature were less until 1985 compared with the second period of 1986 to 2010. Similarly, the changes in mean and summer precipitation in the first 25 years were less compared with 1986 to 2010 (Table 3) and (Fig. 5).

### Long-term Change Analysis in Gilgit River Flows

Trend analysis of Gilgit temperature and river flows from 1961 to 2010 revealed that – due to increases in the mean, maximum, and minimum temperatures – flows in the Gilgit increased. Insignificant changes in temperature

Table 3. Change in annual and seasonal mean temperatures (°C) and precipitation (mm) per period of the Gilgit climatic station using Mann-Kendall and Sen’s slope methods.

| Season       | Mean Temperature |         |             | Average Precipitation |         |           |
|--------------|------------------|---------|-------------|-----------------------|---------|-----------|
|              | 1961-2010        | 1961-85 | 1986-2010   | 1961-2010             | 1961-85 | 1986-2010 |
| Annual(J-D)  | 0.45             | 0.27    | <b>0.84</b> | 2.6                   | 0.56    | 2.20      |
| Winter (O-M) | <b>1.11</b>      | -0.13   | <b>1.30</b> | 0.4                   | -1.45   | -0.61     |
| Summer (A-S) | -0.33            | 0.48    | 0.53        | 4.7                   | 0.81    | 4.74      |
| Winter (DJF) | <b>1.57</b>      | 0.03    | <b>0.95</b> | 0.6                   | -8.01   | 5.58      |
| Spring (MAM) | <b>1.11</b>      | 0.68    | <b>2.59</b> | 2.0                   | 17.86   | 8.90      |
| Summer (JJA) | <b>-1.34</b>     | 0.24    | 0.14        | 4.6                   | -0.97   | -0.62     |
| Autumn (SON) | 0.28             | -0.25   | 0.43        | 0.0                   | -5.42   | -1.17     |

Note: Bold and italic values show that the trend is significant at the 95% confidence level.

Table 4. Percentage change in the annual and seasonal flows of the Gilgit River per period using Mann-Kendall and Sen's slope methods.

| Period/Season | Annual (J-D)            | Winter (O-M) | Summer (A-S)            | Winter (DJF) | Spring (MAM)            | Summer (JJA) | Autumn (SON) |
|---------------|-------------------------|--------------|-------------------------|--------------|-------------------------|--------------|--------------|
| 1961-2010     | <b>15.2<sup>+</sup></b> | 6.9          | <b>15.8<sup>+</sup></b> | 3.5          | <b>54.8</b>             | 10.9         | 12.4         |
| 1961-85       | -8.5                    | <b>-10.7</b> | -7.9                    | <b>-10.8</b> | 13                      | -8.9         | <b>-16.7</b> |
| 1986-2010     | 15                      | 5.0          | 15.1                    | 1.3          | <b>42.3<sup>+</sup></b> | 11.3         | 15.3         |

Note: Bold and italic and bold and (+) sign values show that the trend is significant at the 95% and 90% confidence levels, respectively.

and precipitation occurred during the first 25 years (1961 to 1985), but after 1985 significant changes in both temperature and precipitation were observed, and flows increased. Table 4 shows that annual and seasonal flows decreased from 1961 to 1985, but rapid increases in flows were observed after 1985.

#### Calibration and Validation of the Snowmelt Runoff Model

The SRM was applied in this study on the Gilgit catchment for estimating the relative contributions of snow/glacier melt and precipitation to stream flow. The SRM is basically useful where snow is the dominant factor and it gives the combined zonal melt depth (cm) produced by both snowmelt and glacier melt. So it is not possible to distinguish between the snowmelt and glacier melt. However, we can estimate (snow+glacier) melt and rainfall contribution separately by using the modelling framework. The study area was divided into six equal elevation zones, and zone-wise simulation was applied. The relative contribution from each zone was estimated through a modelling framework.

The final decade of the study period was more critical due to climate change and was used for calibrating and validating the SRM, which was calibrated over four years (2001 to 2004). The range of parameters obtained from the calibration was validated successfully over six years (2005 to 2010). The daily precipitation does not significantly affect the discharges in high-altitude basins. The SRM is designed to work under scarcity of data so that in the absence of precipitation data it encounters the snow-covered area to compute the runoff. The discharge obtained from SRM is mainly affected by temperature and less affected by precipitation [40]. Thus, daily average temperature and precipitation data from the high altitude and low altitude climatic stations of the Gilgit catchment were used as inputs in all SRM elevation zones. The parameters necessary for calibration were extracted from past data analyses and some parameters from past studies [10, 35, 40, 52].

The temperature lapse rate value of 0.64°C/100 m was computed for the Gilgit River basin between the lowest elevation climate station (Gilgit, 1,430 m) and the highest elevation climate station (Yasin, 3,150 m). The temperature was extrapolated from low to high elevation to obtain the lapse rate. The value of critical temperature (Tcrit) was

calculated from the long-term temperature and precipitation records. This parameter decides whether the measured precipitation is snow or rain. The value for Tcrit was selected as 2°C. If  $T < T_{crit}$  there is a chance of snowfall. This value is more important in the accumulation period as compared to the ablation period. The value of degree day factor is not constant, and varies according to changing snow properties during snowmelt season. In glaciated basins, the value of degree-day factor exceeds 0.6 cm C<sup>-1</sup>d<sup>-1</sup> at the end of the summer season when ice is exposed [53]. As Gilgit is a glaciated basin, initially 0.1cm C<sup>-1</sup>d<sup>-1</sup> value of degree-day factor was used and 0.65 cm C<sup>-1</sup>d<sup>-1</sup> was used during the peak ablation period. The rainfall (Cr) and snow (Cs) runoff coefficients describe the percentage of rainfall and snowfall converted to runoff. These values were determined from available long-term precipitation and runoff data. The values of runoff coefficients used in SRM ranged from 0.03 to 0.30. The value of the rainfall contributing area (RCA) in the model was 0 from October to April because in winter the rainfall is retained by the snow and ice. RCA value of 1 was used for the snowmelt period because this is the period of snow ripening, and during this period all the rainfall on the snow-covered area converted to runoff. The values of recession coefficients Xc and Yc describe the amount of discharge contribution from the previous day's snowmelt

Table 5. SRM Parameter values used in the model.

| Parameter  | Parameter Values                        |
|--|---|
| Temperature Lapse Rate (°C/100 m)                        | 0.64                                    |
| Tcrit (°C)   | 2                                       |
| Degree day factor (cm °C <sup>-1</sup> d <sup>-1</sup> ) | 0.1-0.65                                |
| Lag time (hrs)   | 18 hrs                                  |
| Runoff coefficient for snow                              | 0.03-0.26                               |
| Runoff coefficient for rain                              | 0.05-0.30                               |
| Rainfall contributing area                               | RCA = 0 -1                              |
| Reference elevation                                      | 3060 m                                  |
| Initial discharge  | 85.47 cumec                             |
| Rainfall threshold                                       | 6.0 cm                                  |
| Recession coefficients                                   | Xcoeff. = 0.95-0.99 and Ycoeff. = 0.001 |

on a given day. Recession coefficients were taken from past studies [40]. They calculated recession coefficients for the Hunza River basin, which is adjacent to Gilgit catchment. Due to similarities in topography and climate, those recession coefficients were used in SRM with little adjustment. The details of the parameters were used in the calibration (Table 5).

### Results and Discussion

#### Future Trend Analysis under Representative Concentration Pathway (RCP) Scenarios

The RCP 4.5 and RCP 8.5 scenarios were selected to estimate the future change in climatic parameters and, ul-

timately, on future runoff. The projected data for Gilgit and other climatic stations was collected with 25 km resolution from the Pakistan Meteorological Department’s (PMD) Numerical Modeling Group of the Research and Development Division. PMD downscaled CCSM4 GCM data at 25- and 50 km resolution using the statistical method from 2011-2100. The projections were made over all of Pakistan.

Mann-Kendall and Sen’s slope methods were applied on the time series data of the RCP 4.5 and 8.5 scenarios. The results are described in this section.

Figs 6(a-c) show the overall changes in the annual, summer, and winter temperatures, respectively, under the RCP 4.5 scenario, whereas Figs. 6(d-f) show the overall changes in the annual, summer, and winter temperatures, respectively, under the RCP 8.5 scenario. RCP 4.5 is a

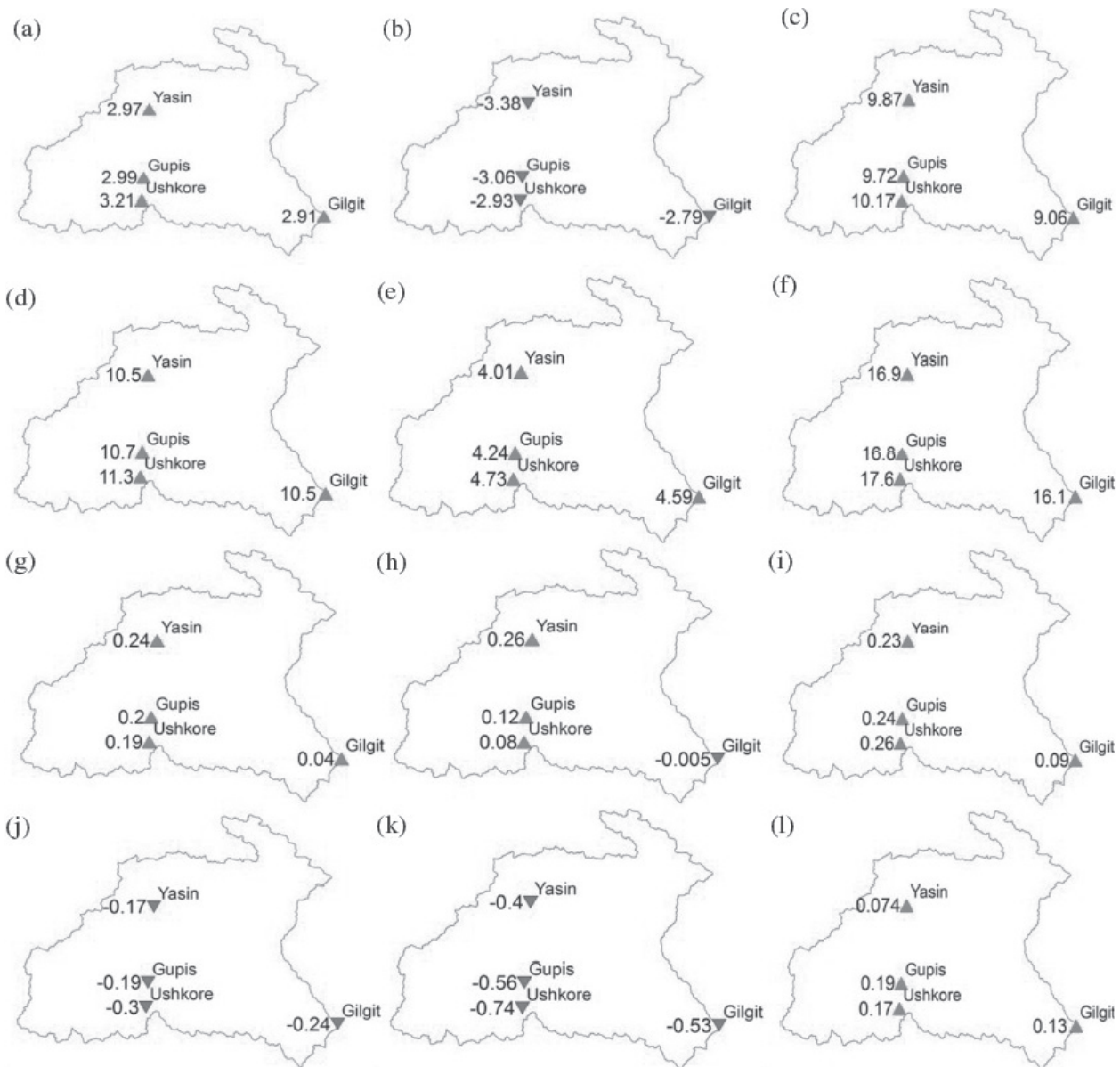


Fig. 6. a-c) show temperature and g-i) show precipitation trends of annual, summer, and winter, respectively, under RCP 4.5 scenario. d-f) show temperature and j-l) show precipitation trends of annual, summer, and winter, respectively, under RCP 8.5 scenario of Gilgit catchment in 90 years from 2011 to 2100.

medium scenario, according to which radiative forcing will decrease before 2100 with proper management. The red sign shows a decreasing trend, and the green sign shows an increasing trend in climatic parameters (Fig. 6). The results obtained from the RCP 4.5 scenario revealed that the average annual temperature will increase by approximately 3°C in 90 years, from 2011 to 2100, in the Gilgit catchment. This trend was significant at  $\alpha < 0.05$  for all climatic stations, with a change rate of 0.033°C year<sup>-1</sup>. It was observed that at all four climatic stations, the summer temperatures will decrease by approximately -2.79°C, -3.38°C, -3.06°C, and -2.93°C at the Gilgit, Yasin, Gupis, and Ushkore stations, respectively, from 2011 to 2100. This decreasing trend was significant at the 95% confidence level or  $\alpha < 0.05$ . [54] observed greater increase in winter minimum temperature as compared to summer maximum temperature from 2000-2011 in the Shigar River Basin, a sub-catchment of UIB of Pakistan. [55] found a contrast between winter and summer temperatures with significant increase in winter mean and maximum temperatures and a constant decrease in summer mean and minimum temperatures from 1961 to 2000 in sub-catchments of UIB. Such a decrease in summer and increase in winter is possible because the climatic variables differ vastly across the region and between the seasons [51].

It was further observed in the RCP 4.5 scenario that the increase in winter temperature will be greater than that in summer and annual temperatures. On average, the winter temperature will increase by 9.70°C in the Gilgit catchment from 2011 to 2100; this trend was also significant at  $\alpha < 0.05$ , with a change rate of 0.107°C year<sup>-1</sup>. Figs 6(d-f) represent the trends in the annual and seasonal temperatures of the Gilgit catchment under RCP 8.5, which is the overshooting scenario. According to this scenario, greenhouse gases will rise to an extreme level [51]. The average annual temperature in Gilgit will increase by approximately 10°C to 11°C at all four climatic stations of the Gilgit catchment from 2011 to 2100. The trend was significant at  $\alpha < 0.001$ , with a change rate of 0.12°C year<sup>-1</sup>. Since 1960, across Southeast Asia temperatures had increased 0.14 to 0.20°C per decade. The number of hot days and warm nights had increased subsequently [51]. Such an extreme change in temperature is possible, as in the Karakoram mountain region, where most of the glaciers are covered with thick debris. The percentage of debris-covered glaciers in the UIB is 10% to 15% of the total perennial snow and glacier cover area [18]. Moreover, climate variability and trends differ enormously across the region and between seasons [51]. So temperature and precipitation trends can vary between seasons and from one station to another especially in highly elevated basins.

Fig. 6e) represents the change in the summer average temperature of the Gilgit catchment from 2011 to 2100 under the RCP 8.5 scenario. It was found that the summer temperature will increase by approximately 4°C (on average) in the Gilgit catchment from 2011 to 2100; this trend was significant at the 95% confidence level, with a change rate of 0.044°C year<sup>-1</sup>. We also observed that under

the RCP 8.5 scenario the winter temperature at all climatic stations will increase by approximately 16°C to 17°C from 2011 to 2100. This trend was also significant at  $\alpha < 0.05$ , with a change rate of 0.189°C year<sup>-1</sup> (Fig. 6f).

Figs 6(g-i) show the changes in annual, summer, and winter precipitation, respectively, under the RCP 4.5 scenario from 2011 to 2100 in the Gilgit Catchment. Annual precipitation will increase by a negligible 0.2 mm from 2011 to 2100; this trend was insignificant. Similarly, summer precipitation will also increase at three climatic stations of the Gilgit catchment (except at Gilgit) from 2011 to 2100. Winter precipitation will also increase from 2011 to 2100 in the Gilgit catchment. However, this trend was insignificant and the change was negligible (Fig. 6i).

Figs 6(j-l) represent the changes in annual, summer, and winter precipitation, respectively, under the RCP 8.5 scenario from 2011 to 2100. We found that annual and summer precipitation will decrease from 2011 to 2100; this trend was insignificant. In contrast, winter precipitation will increase from 2011 to 2100 under the RCP 8.5 scenario; however, this trend was also insignificant.

### Snow Cover Dynamics in Gilgit River Basin

Snow cover dynamics were performed basin-wide from 2001 to 2012. The results showed that during accumulation period about 90-95% area of Gilgit catchment is covered by seasonal snow and ice, while during the ablation period all the seasonal snow is melted till August and its value dropped to 10 to 15%. The accumulation period starts in September and snow cover reaches a range of 80-85% in December (Figs 7a-b).

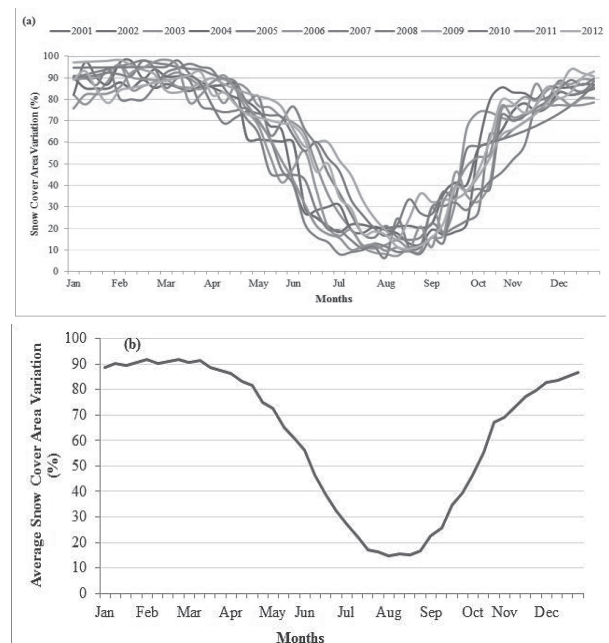


Fig. 7. a) Basin-wide snow cover area variations (2001-12) and b) average (2001-12) basin-wide snow cover area variations in Gilgit catchment using MOD10A2 satellite data.

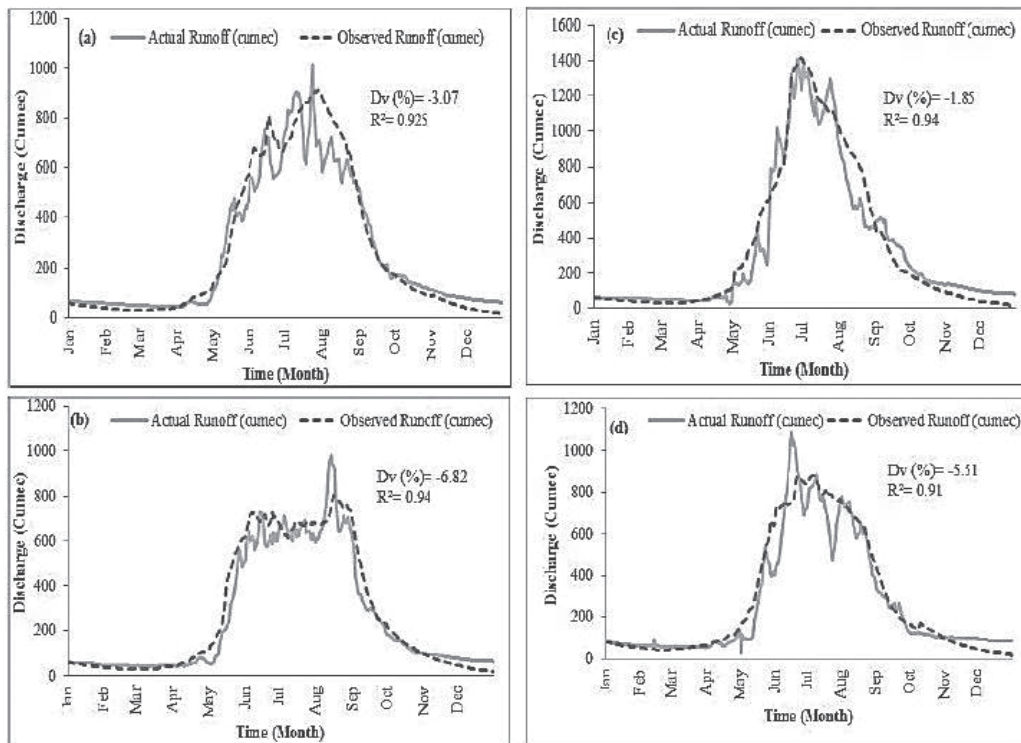


Fig. 8. Calibration of SRM over four hydrological years (2001-04) as shown with figure numbers a-d.

### Calibration of the SRM

The SRM was calibrated for the Gilgit River basin. The daily flow data of the Gilgit stream gauging station were used in the analysis. The SRM model was applied zone wise, and the model was calibrated over four years from 2001 to 2004 (Fig. 8).

Fig. 8 presents a good correlation between the observed and the simulated flows of the Gilgit River during the calibration period, i.e., 2001 to 2004. Table 6 shows that the calibration of the SRM was successful, with Nash-Sutcliffe coefficients of 0.92, 0.94, 0.94, and

0.91, and volume differences of -3.07%, -6.82%, -1.85%, and -5.51% for 2001, 2002, 2003, and 2004, respectively. The values of the Pearson correlation coefficient were strongly correlated and nearly equal to 1 for 2002, 2003, and 2004 (Table 6). The mean absolute error (MAE) measures the average magnitude of the errors in a set of forecasts, despite their direction. The root mean square error (RMSE) is a quadratic scoring rule that measures the average magnitude of the error. Both MAE and RMSE are used to identify the deviations in the errors obtained from a set of forecasts. Lower values of these parameters are better. Findings of the study showed that values of these errors are not high. In other terms, the deviations between observed and forecasted values are reasonable (Table 6).

Table 6. Statistical description of actual and observed flows of the Gilgit River.

| Statistical Parameter           | 2001  | 2002  | 2003  | 2004  |
|---------------------------------|-------|-------|-------|-------|
| Volume Difference, Dv. (%)      | -3.07 | -6.82 | -1.85 | -5.51 |
| Nash-Sutcliffe Coefficient      | 0.92  | 0.94  | 0.94  | 0.91  |
| Pearson Correlation Coefficient | 0.975 | 0.977 | 0.974 | 0.96  |
| Mean Error (Cumec)              | 8.14  | 17.56 | 6.28  | 14.92 |
| Root Mean Square Error (Cumec)  | 72.24 | 62.57 | 95.97 | 80.53 |
| Mean Absolute Error (Cumec)     | 49.17 | 42.02 | 67.79 | 49.16 |
| No. of Observations (N)         | 365   | 365   | 365   | 366   |

### Year-round Simulation of the SRM

The SRM was applied zone wise further after calibration, from 2005 to 2010, over the Gilgit catchment. The results showed that model performance was satisfactory. The results obtained after the year-round simulation are given in Table 7.

Table 7 shows good correlation between the observed and simulated flows of the Gilgit River, with Nash-Sutcliffe coefficients greater than 0.90 from 2005 to 2010 (except for 2006 and 2008, whose coefficient values were 0.89 and 0.84). The volume difference between the observed and the simulated flow ranged from -2.12% to +8.26% (Table 7). The value of the Pearson correlation coefficient was also strong, and it was nearly equal to 1 for the hydrological years of 2005 and 2007. The values of

Table 7. Statistical description of actual and observed flows of the Gilgit River.

| Statistical Parameter           | 2005   | 2006  | 2007  | 2008   | 2009  | 2010   |
|---------------------------------|--------|-------|-------|--------|-------|--------|
| Volume Difference, Dv. (%)      | -2.12  | 1.81  | -2.67 | 5.88   | -2.06 | 8.26   |
| Nash-Sutcliffe Coefficient      | 0.94   | 0.89  | 0.90  | 0.84   | 0.91  | 0.92   |
| Pearson Correlation Coefficient | 0.97   | 0.95  | 0.96  | 0.93   | 0.945 | 0.97   |
| Mean Error (Cumecc)             | 12.57  | 4.27  | 4.53  | -16.08 | 9.66  | -33.71 |
| Root Mean Square Error (Cumecc) | 170.30 | 93.71 | 87.06 | 107.70 | 98.16 | 100.02 |
| Mean Absolute Error (Cumecc)    | 98.77  | 58.75 | 57.17 | 60.58  | 65.44 | 61.02  |
| No. of Observations (N)         | 365    | 365   | 365   | 366    | 365   | 365    |

RMSE and MAE were also satisfactory and showed less deviation between the observed and simulated discharges (Table 7).

Fig. 9a) displays good correlation between the observed and simulated flows of the Gilgit River, with a Nash-Sutcliffe coefficient of 0.91 for the hydrological year of 2009. It showed that most of the precipitation in the Gilgit catchment occurred from January to June, whereas less precipitation occurred from July to December (Fig. 9a). The river runoff reached its peak due to glacier melting and summer rainfall during July and August, after which the recession started. The base flow in the Gilgit River in the non-monsoon period generally remained at approximately 80 m<sup>3</sup>/s to 90 m<sup>3</sup>/s (Fig. 9a).

Fig. 9b) shows the linear regression at the 95% confidence level between the observed and the simulated flows of the Gilgit River for the hydrological years from (2006-10). The average of actual and observed discharge

values from 2006 to 2010 were used in the analysis. There was good correlation with the coefficient of model efficiency of ( $R^2 = 0.974$ ).

The variations of average zonal (snow+glacier) melt depth (cm) from 2006 to 2010 are shown in Fig. 10. The snowmelt runoff model gives the daily snowmelt and rainfall depths in cm. So daily melt obtained from SRM is the sum of both snowmelt and glacier melt. Zones A and B located at low elevation where snow is diminished till May, while Zone E and F having some glaciers where melting continues until October. Melting rate is maximum in July due to the melting of glaciers during the summer months (JJA) due to high temperatures and summer rainfall. Glacier melting abruptly decreased after September due to temperature decreases in the Gilgit catchment (Fig. 10).

*Relative Contribution of Runoff Components to the Total Stream Flow of the Gilgit River*

The SRM converts the snow cover area into daily melt depth. It converts the precipitation into melt depth on the base of critical temperature. Some precipitation is considered to be snowfall and it is added to snowmelt depth while the remaining precipitation is considered to be rainfall and contributes to stream flow separately. The contribution of rain and snow was calculated from each

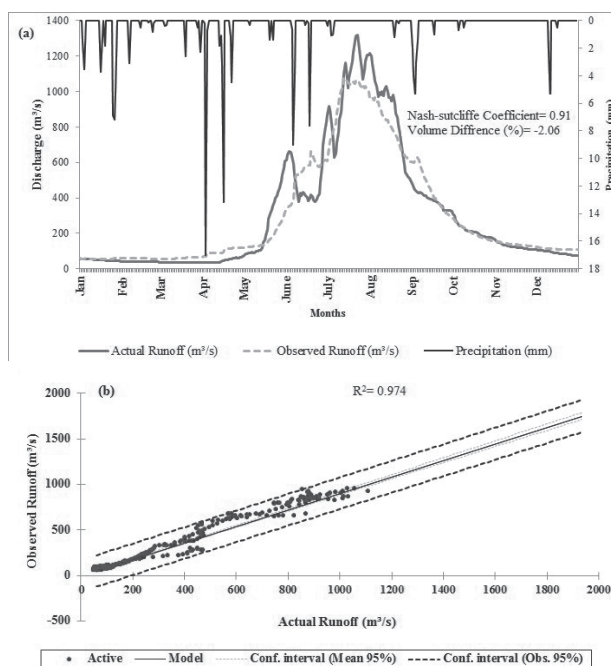


Fig. 9. a) Evaluation of basin-wide SRM application for hydrological year 2009 and b) correlation between average actual and observed runoff for the hydrological years 2006-10.

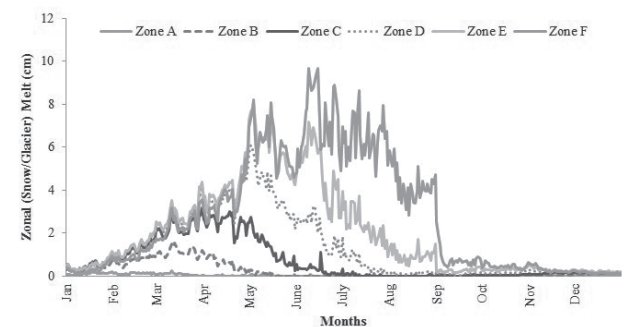


Fig. 10. Variations of average zonal (snow/glacier) melt depth (cm) (2006-10) in Gilgit catchment.

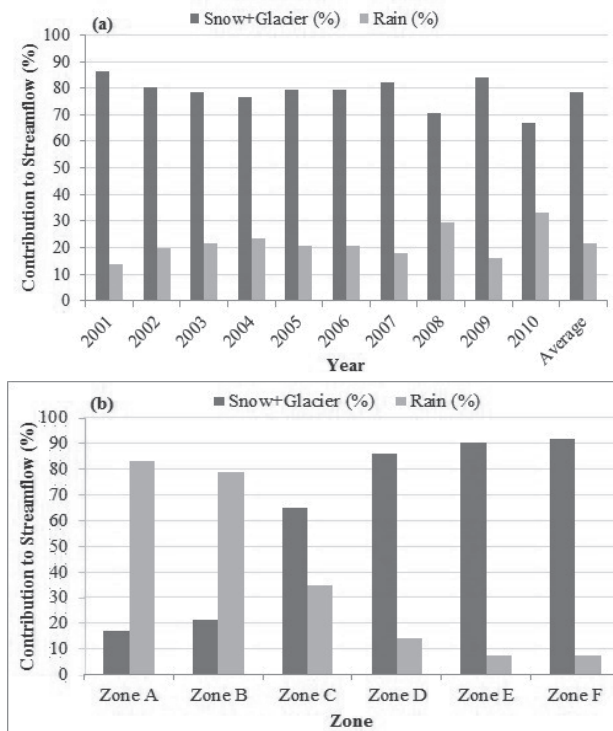


Fig. 11. a) Average basin-wide relative contribution of snow/glacier melt and rainfall to stream flow from (2001-10) and b) average altitude-wise contribution to stream flow from (2001-10) in Gilgit catchment.

zone, then the relative contribution of each component was calculated. The relative contribution of (snow+glacier) melt and rainfall separately was calculated from 2001 to 2010. It was observed that the average contribution of (snow+glacier) melt to stream flow is about 78%, while rainfall is about 22% (Fig. 11a).

Fig. 11b) shows the average zone wise contribution from 2001 to 2010. It is clear from this figure that in zones A and B the contribution of rainfall is about 80%, which is more when compared to snowmelt. From low to high elevation zones the contribution of rainfall is decreased while snow and ice is increased.

### Prediction of Future Flows of the Gilgit River under RCP Scenarios

The snowmelt runoff model was employed to predict the future flows of the Gilgit River under the RCP emission scenarios. The climate change scenarios were developed in the SRM under the RCP 4.5 and 8.5 scenarios.

#### Impact of Increase in Average Annual Temperature on River Flows

According to the RCP 4.5 emission scenario, the average annual temperature of the Gilgit catchment will increase by 3.02°C from 2011 to 2100, whereas according to the RCP 8.5 scenario, the average annual temperature of the Gilgit catchment will increase by 10.76°C by the

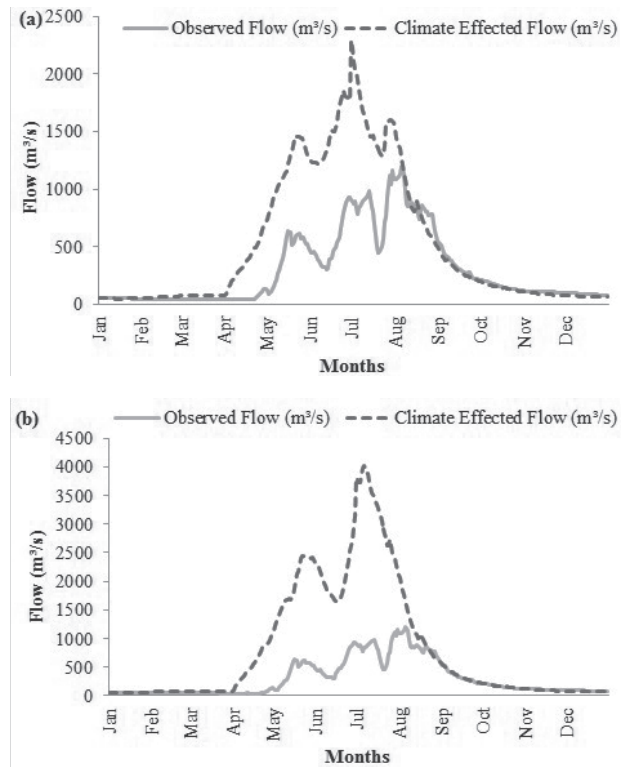


Fig. 12. Monthly discharge simulations in Gilgit River basin under climate change scenarios a) RCP 4.5 and b) RCP 8.5 (2011-00) for the hydrological year 2007.

end of this century. The same parameters were applied in the climate change scenario because calibration of the model is not suitable for climate effect studies because some parameters cannot be meaningfully adjusted to the conditions as described by [56-58]. These average annual temperature values along with DDF and coefficient of snow were used in the SRM as inputs in the climate change scenario. The reason to add degree day factors and coefficients of snow in climate change scenario was because DDF gradually increases with snow density and Cs gives the information about snow cover area and vegetation stage.

RCP 4.5 and 8.5 scenarios were applied over four years from 2007 to 2010 to get the better perspective of climate change impact on river flows. The results obtained from the SRM under the RCP 4.5 scenario revealed that with an increase of 3.02°C in the average annual temperature by the end of this century, average winter, summer, and annual flows will increase by 10.4%, 70.6%, and 67.03%, respectively, as shown in Table 8 and Fig. 12a). We observed that due to the increase in temperature, the seasonal snow will melt earlier, and the glacier melting period will increase; consequently, flows in the Gilgit will increase.

Similarly, the results obtained from the SRM under the RCP 8.5 scenario revealed that with an increase of 10.76°C in the average annual temperature by the end of this century, average winter, summer, and annual flows will increase by 22.5%, 186.7%, and 177.5%, respectively,

Table 8. Percentage flow increase due to the rise in average annual temperatures under the RCP scenarios in the Gilgit River (2011-2100).

| Emission Scenarios | Year    | Time Period | Average T(C°) | Winter Flow (%) | Summer Flow (%) | Annual Flow (%) |
|--------------------|---------|-------------|---------------|-----------------|-----------------|-----------------|
| RCP 4.5            | 2007    | 2011-2100   | 3.02          | 13.63           | 78.74           | 75.80           |
| RCP 4.5            | 2008    | 2011-2100   | 3.02          | 7.9             | 88.10           | 81.52           |
| RCP 4.5            | 2009    | 2011-2100   | 3.02          | 11.78           | 87.25           | 83.39           |
| RCP 4.5            | 2010    | 2011-2100   | 3.02          | 9.83            | 74.56           | 71.25           |
| RCP 4.5            | Average | 2011-2100   | 3.02          | 10.46           | 70.69           | 67.03           |
| RCP 8.5            | 2007    | 2011-2100   | 10.76         | 22.12           | 178.87          | 171.76          |
| RCP 8.5            | 2008    | 2011-2100   | 10.76         | 19.57           | 210.43          | 194.90          |
| RCP 8.5            | 2009    | 2011-2100   | 10.76         | 20.56           | 186.47          | 177.98          |
| RCP 8.5            | 2010    | 2011-2100   | 10.76         | 27.75           | 171.25          | 165.43          |
| RCP 8.5            | Average | 2011-2100   | 10.76         | 22.5            | 186.75          | 177.51          |

as shown in Table 8 and Fig. 12b). To accommodate such a large water supply, in near future there will be a need to construct a new storage reservoir.

#### *Impact of Increase in Cryosphere Area on River Flows*

According to the IPCC AR5 report, annual total wet day precipitation has increased by 22 mm, while an extreme day's precipitation has increased by 10 mm per decade in Southeast Asia, but variability in climatic trends between the seasons and across the region has been found [51]. Due to an increase in precipitation the cryosphere area in high altitude basins like Gilgit will also increase. On this base, two scenarios were developed to encounter the impacts of an increase in the cryosphere area on stream flows. Two scenarios (i.e., 10% and 20% increases in the cryosphere area) were used in SRM to estimate the change

Table 9. Impact of increase in cryospheric area on stream flows of Gilgit River basin.

| Year    | Scenario (% increase in cryosphere area) | Time Period | Annual Flow (%) |
|---------|--|-------------|-----------------|
| 2007    | +10                                      | 2011-50     | 19.5            |
| 2008    | +10                                      | 2011-50     | 26.7            |
| 2009    | +10                                      | 2011-50     | 22.1            |
| 2010    | +10                                      | 2011-50     | 13.9            |
| Average | -  | -           | 20.55           |
| 2007    | +20                                      | 2011-75     | 37.2            |
| 2008    | +20                                      | 2011-75     | 42.2            |
| 2009    | +20                                      | 2011-75     | 44.3            |
| 2010    | +20                                      | 2011-75     | 26.10           |
| Average | -  | -           | 37.45           |

in Gilgit stream flows. Table 9 shows that if the cryosphere area is increased to 10% until 2050 due to an increase in precipitation, then the average annual flow will increase by 20%. And if snow cover is increased to 20% until 2075 then average annual flow in the Gilgit will increase to 37.5%. The analysis was undertaken over four years (2007 to 2010) to get a better understanding of stream flow under climate change (Table 9 and Figs 13a-b).

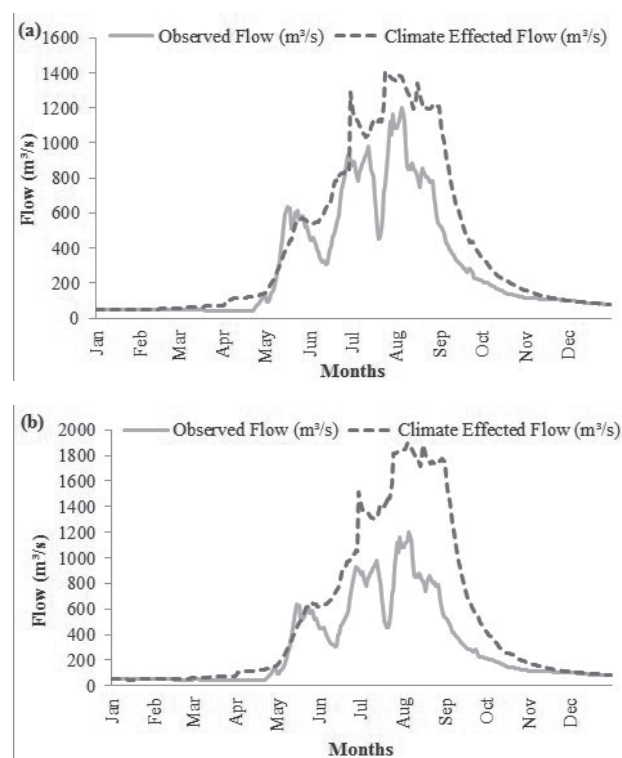


Fig. 13. Monthly discharge simulations in Gilgit River basin under climate change scenarios a) 10% increase in cryosphere area until 2050 and b) 20% increase in cryosphere area till 2075 for the hydrological year 2007.

## Conclusions

The annual and seasonal maximum, minimum, and average temperatures have increased significantly since 1986 in the Gilgit catchment. The increase in spring (MAM) flows was high compared with the annual and other seasonal flows due to significant increases in spring (MAM) temperature. Thus, spring temperature and flows were interrelated.

The trend analysis under the RCP emission scenarios showed that the temperature in the Gilgit catchment will increase significantly (approximately 3°C to 10°C) due to the extreme increase in the concentrations of greenhouse gases in the atmosphere by the end of the 21<sup>st</sup> century. The Gilgit catchment is covered with glaciers, and the seasonal snow and most of the glaciers are debris covered. Therefore, the increase in the amount of incident radiation as mentioned in [51] will increase the temperature in the surroundings, and the glacier melt rate will increase. Moreover, temperature and precipitation vary across the region and also between the seasons mentioned in [51]. The possibility of such an extreme rise in temperature under the RCP scenarios cannot be neglected.

The SRM can efficiently be used for the simulation of daily discharges in snow and glacier-covered catchments in the Upper Indus Basin. Cryospheric data from MODIS can be confidently used for the computation of the snow water equivalent. Seasonal snow is the major contributor to the stream flows of the Gilgit River, followed by rainfall and glacier melt. The SRM predicted a significant increase in the Gilgit River flows under the RCPs scenarios by the end of the 21<sup>st</sup> century. The increase in temperature will result in an increase in the melting of permanent snow in summer (JJA). Pakistan is located in the monsoon belt, and heavy rainfall occurs during summer (JJA). Therefore, flooding conditions will be created in Gilgit and its adjoining rivers due to both glacier melt and summer rainfall. The construction of new storage reservoirs to accommodate such a large amount of runoff is inevitable.

## Acknowledgements

This work was funded by the National Natural Science Foundation of China (grant Nos. 41421061, 41225002, and 41190081). This financial support is gratefully acknowledged and appreciated. The authors are thankful to the Pakistan Meteorological Department and the Pakistan Water and Power Development Authority for providing data for this study.

## References

- BOOKHAGEN B., BURBANK D.W. Towards a complete Himalayan hydrologic budget: the spatiotemporal distribution of snow melt and rainfall and their impact on river discharge. *J. of Geophys. Res.*, **115**, F03019, **2010**.
- IMMERZEEL W.W., PELLICCIOTTI F., SHRESTHA A.B. Glaciers as a proxy to quantify the spatial distribution of precipitation in the Hunza basin. *Mountain Research and Development*, **32**, 30, **2012**.
- IMMERZEEL W.W., PELLICCIOTTI F., BIERKENS M.F.P. Rising river flows throughout the twenty first century in two Himalayan glacierized watersheds. *Nature Geoscience*, **6**, 742, **2013**.
- ARCHER D.R. Contrasting hydrological regimes in the upper Indus basin. *J. Hydrol.*, **274**, 198, **2003**.
- MUKHOPADHYAY B., KHAN A.A. Quantitative assessment of the genetic sources of the hydrologic flow regimes in Upper Indus Basin and its significance in a changing climate. *Journal of Hydrology*, **509**, 549, **2014a**.
- DIMRI A.P., YASUNARI T., WILTSHIRE A., KUMAR P., MATHISON C., RIDLEY J., MATHISON C., JACOB D. Application of regional climate models to the Indian winter monsoon over the western Himalayas. *Science of Total Environment*, **468**, **2013**.
- DIMRI A.P., CHEVUTURI A. Model sensitivity analysis study for western disturbances over the Himalayas. *Meteorology and Atmospheric Physics*, **123**, 155, **2014**.
- RASUL G., MAHMOOD A.S., KHAN A. Vulnerability of the Indus Delta to Climate Change in Pakistan. *Pakistan Journal of Meteorology*, **8** (16), 89, **2012**.
- AKHTAR M., AHMAD N., BOOIJ M.J. The impact of climate change on the water Resource of Hindu Kush–Karakorum–Himalaya region under different glacier coverage scenarios. *J. Hydrol.*, **355**, 148, **2008**.
- IMMERZEEL W.W., BEEK L.P.H., BIERKENS M.F.P. Climate change will affect the Asian water towers. *Science*, **328**, 1382, **2010**.
- KOTHAWALE D.R., REVADEKAR J.V., KUMAR K.R. Recent trends in pre-monsoon daily temperature extremes over India. *Journal of Earth System Science*, **119**, 51, **2010**.
- BOCCHIOLA D., DIOLAUTI G. Recent (1980-2009) evidence of Climate Change in the Upper Karakoram, Pakistan. *Theoretical and Applied Climatology*, **113**, 611, **2013**.
- HEWITT K. The Karakoram anomaly? Glacier expansion and the elevation effect, Karakoram Himalaya. *Mountain Research and Development*, **25**, 332, **2005**.
- GARDELLE J., BERTHIER E., ARNAUD Y. Slight mass gain of Karakoram glaciers in the early twenty-first century. *Nature Geoscience*, **5** (5), 322, **2012b**.
- BOLCH T., KULKARNI A., KÄÄB A., HUGGEL C., PAUL F., COGLEY J.G., STOFFEL M. The State and Fate of Himalayan glaciers. *Science (New York, N.Y.)*, **336**, 310, **2012**.
- SCHMIDT S., NÜSSER M. Changes of high altitude glaciers from 1969 to 2010 in the Trans-Himalayan Kang Yatze Massif, Ladakh, Northwest India. *Arctic, Antarctic, and Alpine Research*, **44**, 107, **2012**.
- MATSUO K., HEKI K. Time Variable ice Loss in Asian High Mountains from the Satellite gravimetry. *Earth and Planetary Science Letters*, **290** (1-2), 30, **2010**.
- HEWITT K. Glacier change, concentration, and elevation effects in the Karakoram Himalaya, Upper Indus Basin. *Mountain Research and Development*, **31** (3), 188, **2011**.
- SARIKAYA M.A., BISHOP M.P., SHRODER J.F., OLSENHOLLER J.A. Space based observations of Eastern Hindu-Kush glaciers between 1976 and 2007, Afghanistan and Pakistan. *Remote Sensing Letters*, **3** (1), 77, **2012**.
- PARRY M.L., CANZIANI O.F., PALUTIKOF J.P., LINDEN P.J., HANSON C.E. Climate Change 2007 Impacts, Adaptation and Vulnerability: Working Group II Contribution to the Fourth Assessment Report of the IPCC

- Intergovernmental Panel on Climate Change (Cambridge: Cambridge University Press), **2007**.
21. ADAM J.C., HAMLET A.F., LATTENMAIER D.P. Implications of Global Climate Change for Snowmelt Hydrology in the Twenty First Century. *Hydrological Process*, **23**, 962, **2009**.
  22. PANDAY P.K., WILLIAMS C.A., FREY K.E., BROWN M.E. Snowmelt runoff modeling in the Tamor River Basin in the eastern Nepalese Himalaya. Department of Geography, Clark University, 950 Main Street, Worcester, MA 01610, **2010**.
  23. KHATTAK M.S., BABEL M.S., SHARIF M. Hydro-meteorological trends in the upper Indus River basin in Pakistan. *Climate Research*, **46**, 103, **2011**.
  24. SCHERLER D., BOOKHAGEN B., STRECKER M.R. Spatially variable response of Himalayan glaciers to climate change affected by debris cover. *Nature Geoscience*, **4**, 156, **2011**.
  25. COGLEY J.G. A more complete version of the world glacier inventory. *Annals of Glaciology*, **50**, 32, **2009**.
  26. Kargel J.S., Cogley J.G., Leonard G.J., Haritashya U., Byers A. Himalayan glaciers: the big picture is a montage. *Proceedings of the National Academy of Sciences of the United States of America*, **108** (36), 14709, **2011**.
  27. BASH E.A., MARSHALL S.J. Estimation of Glacier melt Contributions to the bow River, Alberta, Canada, using a radiation Temperature Melt Model. *Annals of Glaciology*, **55**, 139, **2014**.
  28. AGARWAL A., BABEL M.S., MASKEY S. Analysis of future precipitation in the Koshi river basin, Nepal. *Journal of Hydrology*, **513**, 422, **2014**.
  29. ZEMP M., HOELZLE M., HAEBERLI W. Six decades of glacier mass balance observations: a review of the world monitoring network. *Annals of Glaciology*, **50** (50), 101, **2009**.
  30. FUJITA K., NUIMURA T., YAMAGUCHI S., SHARMA R. Temporal changes in elevation of the debris-covered ablation area of Khumbu Glacier in the Nepal Himalaya since 1978. *Arctic, Antarctic, and Alpine Research*, **43** (2), 246, **2011**.
  31. MAIDMENT D.R. "GIS and Hydrologic Modeling", Plenary Speech at the 2nd International Conference on Integrating Geographic Information Systems and Environmental Modeling, Breckenridge, Colorado, **1993**.
  32. SORMAN A.A., SENSOY A., TEKELI A.E., SORMAN A.U., AKYUREK Z. Modeling and forecasting snowmelt runoff process using the HBV model in the eastern part of Turkey. *Hydrological Process*, **23** (7), 1031, **2009**.
  33. SHAKIR A.S., REHMAN H., EHSAN S. Climate Change Impact on River Flows in Chitral Watershed. *Pakistan journal of Engineering & Applied Sciences*, **7**, 12, **2010**.
  34. WMO. Intercomparison of models of snowmelt runoff. *Operational Hydrology Report 23*, World Meteorological Organization, Geneva, Switzerland, WMO -No.646, **1986**.
  35. HOCK R. Temperature index melt modelling in mountain areas. *Journal of Hydrology*, **282** (1-4), 104, **2003**.
  36. SEIDEL K., MARTINEC J. Noaa/Avhrr Monitoring Of Snow Cover for Modeling Climate-Affected Runoff in Ganges and Brahmaputra Rivers. *Proceedings of EARSeL-LISSIG-Workshop Observing our Cryosphere from Space*, Bern, March 11-13, **2002**.
  37. PRASAD V.H., ROY P.S. Estimation of Snowmelt runoff in Beas basin, India. *Geocarto International*, **20** (2), 41, **2005**.
  38. MATEEN H. Snowmelt Runoff Investigation in River Swat using Snowmelt Runoff Model, Remote Sensing and GIS Techniques. M.Sc. Thesis, International Institute for Geo-Information Science and Earth Observation Enschede, the Netherlands, **2008**.
  39. GEORGIEVSKY M.V. Application of the Snowmelt Runoff Model in the Kuban River basin using MODIS satellite images. *Environmental Research Letters*, **4**, 1, **2009**.
  40. TAHIR A.A., CHEVALLIER P., ARNAUD Y., NEPPEL L., AHMAD B. Modeling Snowmelt-Runoff under climate scenarios in the Hunza River basin, Karakoram Range, Northern Pakistan. *Journal of Hydrology*, **409** (1-2), 104, **2011b**.
  41. WMO. Simulated real-time intercomparison of hydrological models. *Operational Hydrology Report 38*, WMO, Geneva, Switzerland, **1992**.
  42. LI X., WILLIAMS M.W. Snowmelt runoff modelling in an arid mountain watershed, Tarim Basin, China. *Hydrological Process*, **22**, 3931, **2008**.
  43. MARTINEC J., RANGO A., ROBERTS R. Snowmelt-Runoff Model (SRM) user's manual. USDA Jornada Experimental Range, New Mexico State University, Las Cruces, NM 88003, USA, **2007**.
  44. RANGO A., MARTINEC J. Predictions for snow cover, glaciers and runoff in a changing climate. *Hydro meteorological Prediction*, **277**, 2008.
  45. SIRGUEY P., MATHIEU R., ARNAUD Y., FITZHARRIS B.B. Seven years of snow cover monitoring with MODIS to model catchment discharge in New Zealand. In: *IEEE International Geoscience and Remote Sensing Symposium*, Cape Town, 863, **2009**.
  46. NAFIS A., DERYCK O., LODRICK. Indus River, Asia; physical features. Article from the Encyclopaedia Britannica. <http://www.britannica.com/286872/Indusriver,2007&2009>.
  47. HASHMI A.A., SHAFIULLAH A. Agriculture and Food Security. Planning & Development Department, Northern Areas of Pakistan, **2003**.
  48. HUA H.X., JIAN W., HONG-YI L. Evaluation of the NDSI Threshold Value in Mapping Snow Cover of MODIS – A Case Study of Snow in the Middle Qilian Mountains. *Journal Of Glaciology And Geocryology*, **30**, 132, **2008**.
  49. TEKELIA A.E., AKYUREK Z., SORMAN A.A., SENSOY A., SORMANA A.U. Using MODIS snow cover maps in modelling snowmelt runoff process in the eastern part. *Remote Sensing of Environment*, **97**, 216, **2005**.
  50. HU Y., MASKEY S., UHLENBROOK S. Trends in temperature and rainfall extremes in the Yellow River source region, China. *Climatic Change*, **110**, 403, **2012**.
  51. IPCC: Summary for Policymakers. In: *Climate Change 2013: The Physical Science Basis. Contribution of Working Group I to the Fifth Assessment Report of the Intergovernmental Panel on Climate Change* [Stocker T.F., Qin D., Plattner G.K., Tignor M., Allen S.K., Boschung J., Nauels A., Xia Y., Bex V., and Midgley P.M (eds.)]. Cambridge University Press, Cambridge, United Kingdom and New York, NY, USA, **2013**.
  52. ZHANG Y., LIU S., DING Y. Observed degree-day factors and their spatial variation on glaciers in western China. *Annals of Glaciology*, **43**, 301, **2006**.
  53. KOTLYAKOV V.M., KRENKE A.N. Investigation of hydrological conditions of alpine regions by glaciological methods. *IAHS Publication*, **138**, 31, **1982**.
  54. IQRA A., IQBAL J., MAHBOOB M.A. Modeling mass balance of Upper Indus Basin glaciers in relation with climatic variability. *Sci. Int. (Lahore)*, **28** (3), 2637, **2016**.
  55. FOWLER H.J., ARCHER D.R. Conflicting Signals of Climatic Change in the Upper Indus Basin. *Journal of Climate*, **19**, 4276, **2005**.

56. KLEMES V. Sensitivity of water resources systems to climate variations. WCP Report 98, Geneva, Switzerland, **1985**.
57. BECKER A., SERBAN P. Hydrological models for water resources system design and operation. Operationalal Hydrology. Report 34, WMO, Geneva, Switzerland, **1990**.
58. NASH L.L., GLEICK J.A. Sensitivity in the stream flow in the Colorado basin to climatic changes. Journal of Hydrology, **125**, 221, **1991**.